

# An Efficient MN-Algorithm for Joint Source-Channel Coding

Haggai KFIR<sup>†</sup>, Eyal SHPILMAN<sup>†</sup> and Ido KANTER<sup>†</sup><sup>†</sup> Minerva Center and Department of Physics, Bar-Ilan University Ramat-Gan, 52900 Israel  
E-mail: kfirha1@mail.biu.ac.il, shpilme@mail.biu.ac.il, kanter@mail.biu.ac.il

## Abstract

Belief Propagation (BP) decoding of LDPC codes is extended to the case of Joint Source-Channel coding. The uncompressed source is treated as a Markov process, characterized by a transition matrix,  $T$ , which is utilized as side information for the Joint scheme. The method is based on the ability to calculate a Dynamical Block Prior (DBP), for each decoded symbol separately, and re-estimate this prior after every iteration of the BP decoder. We demonstrate the implementation of this method using MacKay and Neel's LDPC algorithm over  $GF(q)$ , and present simulation results indicating that the proposed scheme is comparable with Separation scheme, even when advanced compression algorithms (such as AC, PPM) are used. The extension to 2D (and higher) arrays of symbols is straightforward. The possibility of using the proposed scheme without side information is briefly sketched.

## 1. INTRODUCTION

The Shannon separation theorem [1, 2], states that source coding and channel coding can be performed separately and sequentially, while maintaining optimality. However, this is true only in the case of asymptotically long blocks of data. Thus, considerable interest has developed in various schemes of joint source-channel coding, where the inherent redundancy of the source is utilized for error correction, possibly with the aid of some side information (see, for instance, [3]). Combining the two processes may be motivated by reducing the total complexity of the procedure, and by some gain in the overall performance. Moreover, some uncompressed files (e.g. bitmap, text) are expected to be resilient to single bit errors, which may corrupt entire blocks in the case of the Separation scheme.

Shannon's lower bound for the channel capacity of a binary symmetric channel (BSC) with flip probability  $f$ , bit error rate  $p_b$  and source entropy  $H(src)$  per bit

is given by [1]:

$$C = \frac{1 - H_2(f)}{H(src) - H_2(p_b)}, \quad (1)$$

where  $H_2(x) = -x \log_2(x) - (1-x) \log_2(1-x)$ , is the entropy of  $x$ , and the capacity,  $C$ , is the maximal ratio between the source length  $k$  and the transmitted length  $m$ .

In this paper we propose an extension of the Low-Density-Parity-Check codes (LDPC) [4] decoding algorithm, primarily designed for i.i.d. sequences, to the case of uncompressed data. Our approach is to regard the source sequence,  $\{s_n\}$ , as driven from some memoryless stationary Markov process with a finite alphabet  $s_n \in \{0, 1, 2, \dots, q-1\}$ , and transition matrix  $T$  of dimensions  $q \times q$ , that describes the probability of transition from symbol  $i$  to symbol  $j$ :  $t_{ij} = P(s_{n+1} = j | s_n = i)$ . The Markov Entropy (per symbol) of such a process is given by:

$$H = - \sum_{i=1}^q P(i) \sum_{j=1}^q P(j | i) \log_2[P(j | i)], \quad (2)$$

where  $P(i)$  is the stationary solution of the Markov process. The entropy *per bit*,  $H / \log_2 q$ , ( $\log_2 q$  being the number of bits in the binary representation of a symbol) can be utilized as  $H(src)$  in Eq. (1).

Neighboring symbols in a Markov sequence are *correlated*. Hence, information about symbols  $s_{n-1}$  and  $s_{n+1}$ , immediately implies some knowledge about  $s_n$ , too. The main contribution of this work, is a method of incorporating this additional knowledge into the Belief Propagation decoding scheme.

## 2. MN ALGORITHM

Our joint source-channel scheme is based on Mackay and Neel's algorithm (a thorough introduction may be found in [5]), a variant of the earlier Gallager code [4]. Although originally proposed for the binary field, extending the MN algorithm to higher finite fields is straightforward as demonstrated in [6]. The original

This work was supported by the Israel Academy of Science .

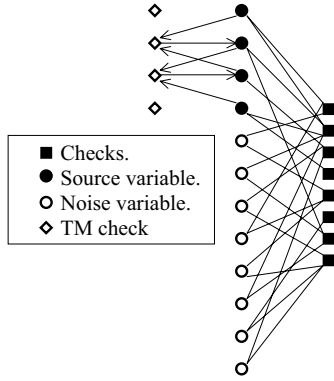


Figure 1: The Dynamic Block Prior visualized as a third layer attached to the bipartite graph of the LDPC code.

motivation for moving to higher fields was reducing the number of edges (and short loops) in the code's graph. For our purpose, this enables us to treat Markov sequences with a richer alphabet, consisting of  $q = 2^i$  symbols ( $i$  being an integer). The algorithm consists of two sparse matrices known both to the sender and the receiver:  $A(m \times k)$ , and  $B(m \times m)$ , where  $k$  is the source block length,  $m$  is the transmitted block length, and the code rate being  $R = k/m$ . All non-zero elements in  $A$  and  $B$  are from  $\{1, 2, \dots, q-1\}$ , and  $B$  must be invertible. Encoding of a source vector  $s$  into a codeword  $t$  is performed (all operations are done over  $GF(q)$ ) by:

$$t = B^{-1} \cdot A \cdot s. \quad (3)$$

$t$  is converted to binary representation and transmitted over the channel. During transmission, noise  $n$  is added to  $t$ , therefore the received vector is  $r = t + n$ . Upon receipt, the decoder reconverts  $r$  back to the original field, and computes the syndrome vector  $z = B \cdot r$ . The receiver then faces the following decoding problem:

$$z = B \cdot (t + n) = B \cdot (B^{-1} \cdot A \cdot s + n) = [AB] \cdot x, \quad (4)$$

where square brackets denote appending of matrices, and  $x$  is a concatenation of  $s$  and  $n$ . The decoding problem can be visualized as a bipartite graph (Fig 1), the elements of  $x$  (circles) and  $z$  (squares) are termed "variable" and "check" nodes, respectively. The edges of the graph correspond to the nonzero elements in  $[AB]$ . For the MN algorithm, one should further distinguish between "source variables" - the  $s$  elements in  $x$  (filled circles), and "noise variables" - the  $n$  elements in  $x$  (empty circles). The decoding problem may be solved using the Belief Propagation (BP) (or sum - product) algorithm [5, 6]. BP is an iterative

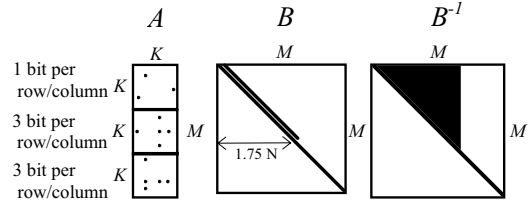


Figure 2: Kanter-Saad [10] construction of the matrices  $A$ ,  $B$ ,  $B^{-1}$  for rate  $1/3$ , black regions denote nonzero elements.

algorithm with two alternating steps, horizontal pass (check  $\rightarrow$  variable messages) and vertical pass (variable  $\rightarrow$  check messages). During the vertical pass, some prior knowledge is assigned to each decoded symbol, according to the assumed statistics (for the i.i.d. case this would simply be:  $Pr(s = j) = 1/q$  for all the source symbols). The key point here is that one can re-estimate and re-assign these priors after every iteration *individually for each decoded symbol* [7]. The outcome of each iteration is an a-posteriori probability  $Q_i^a = Pr(x_i = a)$ , for each symbol (both source and noise). The MN decoder is linear in the size of the source block,  $k$ , with complexity  $O(kqu)$  (per iteration), where  $u$  is the average number of checks per symbol [8, 9].

A proper construction of the matrices  $A$  and  $B$  is crucial in order to ensure nearly capacity-achieving performance. In this work we follow the Kanter and Saad (KS) constructions [10, 11], which are very sparse, simple to construct, and perform very close to the bound. The  $B$  matrix has a systematic construction: diagonal and sub diagonal, which simplifies computation tasks [8, 11, 12]. The KS construction for  $R = 1/3$ ,  $GF(2)$ , is schematically displayed in Fig. 2, black regions denote nonzero elements. Extending the construction to higher  $GF(q)$  is done by randomly replacing the nonzero elements with elements of the corresponding field. Although constructed originally for i.i.d. sources, we successfully used KS matrices for uncompressed sources, however, we mention the possibility of improving the performance by devising better codes.

The MN algorithm is also applicable for the case of an Additive White Gaussian Noise (AWGN) channel [11]. The binary transmitted vector (assumed for simplicity to be  $\pm 1$ ) is corrupted by noise with zero mean and variance  $\sigma^2$ , hence, the received vector,  $r^R$ , is real valued. The *binary* received vector,  $r$ , is determined by hard-decision, namely,  $r_i = +1$  if  $r_i^R > 0$ . The probability of the transmitted bit  $t_i = \pm 1$  is given

by:

$$\begin{aligned} P(t_i = \pm 1 | r_i^R) &= \frac{e^{-(t_i - r_i^R)^2 / 2\sigma^2}}{e^{-(t_i - r_i^R)^2 / 2\sigma^2} + e^{-(t_i + r_i^R)^2 / 2\sigma^2}} \\ &= \frac{1}{1 + e^{-2t_i r_i^R / \sigma^2}}, \end{aligned} \quad (5)$$

and the probability of an error in the  $i^{th}$  hard-decision bit is given by:

$$P(n_i = 1 | r_i^R) = \frac{1}{1 + e^{2|r_i^R|/\sigma^2}}. \quad (6)$$

Eq. (6) is used for calculating a prior for each noise variable. Apart of these modifications, the MN algorithm for an AWGN channel is identical to the BSC case.

The channel capacity for AWGN is given by [2]:

$$C = \frac{1}{2 \cdot H(src)} \log(1 + \frac{1}{\sigma^2}) \quad (7)$$

For binary source messages, (rather than real source messages), however, there exist a tighter bound, [11]:

$$\begin{aligned} C &= \frac{1}{H(src)} (- \int dy P(y) \log P(y) + \\ &\quad \int dy P(y|x = x_0) \log P(y|x = x_0)) \end{aligned} \quad (8)$$

where  $x$  is the transmitted bit,  $x_0 = \pm 1$  and  $y$  is the received (corrupted) bit, with

$$P(y) = \frac{1}{2\sqrt{2\pi\sigma^2}} \left[ e^{-(y-x)^2 / 2\sigma^2} + e^{-(y+x)^2 / 2\sigma^2} \right]. \quad (9)$$

### 3. DERIVING THE DYNAMICAL BLOCK PRIORS

In every iteration of the MN algorithm, a better estimate of each variable node is attained (on average). In this section we shall describe our method of incorporating the statistical knowledge about the source, and these local estimates. Consider three successive symbols  $s_{n-1}, s_n, s_{n+1}$  in a sequence generated by a Markov process with transition matrix  $T$  and alphabet  $GF(q)$ . The probability of a triplet  $a, b, c$  is given by [13]:

$$\begin{aligned} P(a, b, c) &= P(a, b) \cdot P(c|a, b) = P(a, b) \cdot P(c|b) \\ &= \frac{P(a, b)P(b, c)}{P(b)} \end{aligned} \quad (10)$$

where use has been made of the Bayes Rule:  $P(x, y) = P(x) \cdot P(y|x)$ , and the fact that the process is memoryless. Now, given the a-posteriori probabilities for

the first and last symbols in the triplet:  $Q_{n-1}^a = Pr(s_{n-1} = a)$  and  $Q_{n+1}^c = Pr(s_{n+1} = c)$ , one can calculate a prior for the probability that  $s_n = b$ :

$$\begin{aligned} Pr(s_n = b) &= \frac{1}{Z} \cdot \sum_{a,c=1}^q P(a, b, c) \cdot Q_{n-1}^a \cdot Q_{n+1}^c = \\ &= \frac{1}{Z} P(b)^{-1} \left( \sum_{a=1}^q P(a, b) Q_{n-1}^a \right) \left( \sum_{c=1}^q P(b, c) Q_{n+1}^c \right), \end{aligned} \quad (11)$$

where  $Z$  is a normalization constant such that:  $\sum_{b=1}^q Pr(s_n = b) = 1$ . We term Eq. (11) the Dynamical Block Prior (DBP).

The extension of the MN algorithm to the joint source-channel case consists of the following steps:

1. A binary sequence of  $k \cdot \log_2(q)$  bits is converted to  $k$   $GF(q)$  symbols.
2. The encoder measures  $T$  and  $P(a)$  for all the  $q$  symbols over the source, and transmits reliably this side information to the decoder.
3. The source is encoded according to (3), then reconverted to binary representation and transmitted over the BSC.
4. The decoder maps the received signal back to  $GF(q)$ , and performs the regular decoding (4), but after every iteration of the BP, the prior for each source symbol is recalculated according to (11).

The complexity of calculating the  $q$  priors for a single symbol according to the posteriors of its neighbors is reduced from  $q^3$  in the naive calculation, to  $q^2$  by Eq. (11). The decoder's complexity remains linear, with total complexity of  $O(kqu + kq^2)$  per iteration. The above-mentioned procedure may be thought of as adding a layer to the bipartite random graph represented by the matrix  $[AB]$ : The DBP's, Eq. (11), are messages passed only among *source* variable nodes, which are spatially related. In Fig. 1, the diamonds represent this new (directional) layer, which connects neighboring source nodes. We note that the possibility of extending this scheme to Gallager codes is an open question, since the source is not explicitly represented in the graph.

### 4. SIMULATION RESULTS

We report here results for a BSC with rate  $R = 1/3$ , and for an AWGN with rate  $1/4$ , using the corresponding KS constructions for  $A$  and  $B$  devised in [10, 11]. Other rates, constructions and block length were also

Table 1: Simulation results for BSC with rate 1/3.

$q$	$k$	$H$	$f_{sh}$	$f_c$	$f_\infty$
4	5000	0.49	0.266	0.215	0.244
8	3333	0.471	0.271	0.223	0.243
16	2500	0.49	0.266	0.21	0.236

checked. Random vectors of length  $L = 10^4$  bits (9,999 for  $q = 8$ ) were generated by the Markov process, then mapped to a vector in  $GF(q)$  with length  $k = L/\log_2[q]$ , and were encoded and decoded as described in the previous section. For each reported result, at least 1000 sample vectors were generated and transmitted.

#### 4.1. Estimating The Code's Threshold

The threshold for infinite source length,  $k \rightarrow \infty$ , is estimated from the scaling argument of the convergence time, which was previously observed for  $q = 2$  [10, 11]. The convergence time, measured in iterations of the MN algorithm, is assumed to diverge as the level of noise approaches the threshold from below. More precisely, we found that the scaling for the divergence of  $t_{med}$  is *independent of  $q$*  and is consistent with:

$$t_{med}(f) \propto \frac{1}{f_\infty - f} \quad ; \quad t_{med}(\sigma) \propto \frac{1}{\sigma_\infty - \sigma} \quad (12)$$

for a BSC, and an AWGN channel, respectively.

This extrapolation is independent of  $k$  [14] (for  $k \gg 1$ ), so by monitoring  $t_{med}$ , for moderate  $k$ , the threshold can be found by a linear fit. (see the inset of Fig. 3) Note that the estimation of  $t_{med}$  is a simple computational task in comparison with the estimation of low bit error probabilities for large  $k$ , especially close to the threshold. We also note that the analysis is based on  $t_{med}$  instead of the *average* number of iterations, since we wish to prevent the dramatic effect of a small fraction of samples with slow convergence or no convergence.

#### 4.2. BSC Simulations

Some selected results are presented in Table 1. The columns correspond to: the field size  $q$ ; the source length in symbols,  $k$ ; the entropy (per bit) of the source  $H$  [15]; and the corresponding maximal noise  $f_{sh}$  (Eq. (1)); the critical noise,  $f_c$ , up to which the bit error rate  $p_b \leq 10^{-5}$ ; and the threshold,  $f_\infty$ , Eq. (12).

In order to compare the joint and the Separation schemes, the generated samples were concatenated to strings of size  $L = 10^5 - 10^6$  bits, and compressed using

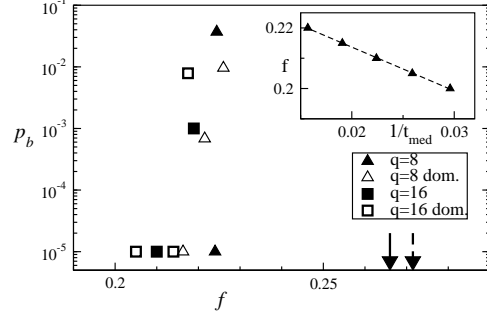


Figure 3: Bit error rate  $p_b$  vs noise level  $f$ , triangles for  $q = 8$ , squares for  $q = 4$ , filled symbols: use of all elements of  $T$  as side information, empty symbols: use of only  $q$  dominant elements of  $T$ . Inset: scaling behavior for median convergence time  $t_{med}$ .  $f_\infty = 0.242$ , is found by linear fit.

two advanced compression algorithms: Prediction by Partial Match (PPM) [16], and Arithmetic Coder (AC) [17]. In Table 2, we preset the compression ratio of the source vectors using each method (%AC, %PPM); the ratio between the compressed sequences and the transmitted blocks,  $m$ , (for the comparison, we use the same transmitted size as for the Joint scheme,  $m = 3k$ ); and the maximal noise level for this new rate for i.i.d. source,  $f_{AC}, f_{PPM}$ . Since we assume an *optimal* decoder, these noise levels should be compared to  $f_\infty$  for the joint scheme. In all cases, the threshold of the proposed Joint scheme for  $k \rightarrow \infty$  is comparable with the Separation scheme. One should recall that these results may be improved by advanced codes. In Fig. 3,  $p_b$  is plotted against the noise level of the channel,  $f$ , for the examples of Table 1. Filled triangles represent  $q = 8$ ; filled squares represent  $q = 16$ ; the empty symbols in this figure refer to an approximation that will be described in the following section. The dashed (full) arrow marks  $f_{sh}$  for  $q = 8$  (16). The inset of Fig. 3 demonstrates the extrapolation of  $f_\infty$  from the convergence time Eq. (12): for  $q = 8$ ,  $f(t_{med})$  is plotted against  $1/t_{med}$ ,  $f_\infty$  is then recovered by a linear fit.

#### 4.3. AWGN Simulations

Binary sequences of length  $k = 10^4$  were generated using the following transition matrix:

$$T = \begin{pmatrix} 0.89 & 0.11 \\ 0.11 & 0.89 \end{pmatrix}, \quad (13)$$

having Markov Entropy  $H(src) = 0.5$ . For rate  $R = 1/4$ , this entropy corresponds to maximal noise, Eq. (8),  $\sigma_{sh} = 2.298$ , (-4.2 Db). The sequences were

Table 2: Critical noise level for Separation scheme using Arithmetic Coder and Prediction by Partial Match compression algorithms.  $f_{AC}$  and  $f_{PPM}$  should be compared to  $f_{\infty}$  in Table 1.

$q$	%AC	$R_{AC}$	$f_{AC}$	%PPM	$R_{PPM}$	$f_{PPM}$
4	58.4%	0.195	0.247	56.6%	0.189	0.25
8	58.1%	0.194	0.248	55.5%	0.185	0.253
16	60.5%	0.201	0.243	59.4%	0.198	0.245

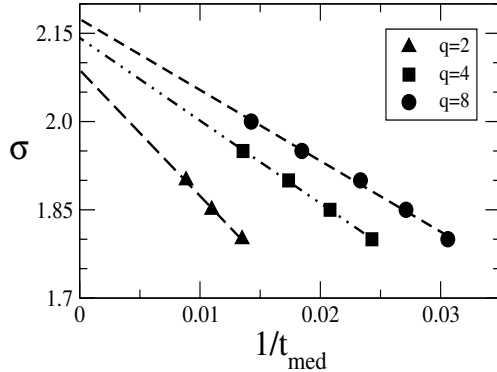


Figure 4: Scaling behavior for AWGN channel:  $\sigma$  is plotted vs.  $1/t_{med}$  for various field sizes,  $q$ .

transmitted over an AWGN channel, using three different fields:  $GF(2)$ ,  $GF(4)$ ,  $GF(8)$ . Fig. 4 presents the scaling behavior, Eq.(12), for these fields (triangles, squares, and circles, respectively). The symbols mark working points with  $p_b \leq 10^{-5}$ , and were used for estimating the corresponding thresholds:  $\sigma_{\infty}(q = 2) = 2.08$ ,  $\sigma_{\infty}(q = 4) = 2.14$ ,  $\sigma_{\infty}(q = 8) = 2.17$ . It is evident that as  $q$  increases, both  $\sigma_c(q)$  and  $\sigma_{\infty}(q)$  improve.

## 5. REDUCING THE AMOUNT OF SIDE INFORMATION

The results of the previous sections indicate that the performance of the presented joint coding is not too far from Shannon's lower bound and, most probably, using an optimized code, the channel capacity can be nearly saturated. However, for a finite block length, the main drawback of our algorithm is the overhead of the header (i.e. the transmitted side information) which must be encoded and transmitted reliably. One has to remember that the size of the header,  $(T)$ , scales with  $q^2$  where the precision of each element is of the

order  $O(\log k)$ . This overhead is especially intolerable in the limit where:  $q^2 \log(k)/k \sim O(1)$ . Note that this is indeed the situation even for very large messages,  $k = 10^6$ , and a symbol size of 8 bits (a "char",  $q = 256$ ).

This point may be tackled by observing that for a process with low entropy, characterized by enhanced repetitions and correlations,  $T$  is dominated by a small number of elements, while the rest of the elements are negligible. We therefore repeated our simulations, using only the  $q$  largest elements in  $T$  as side information. The decoder would then set all other elements in each row of  $T$  equally, to obey the normalization condition  $\sum_j T_{ij} = 1$ . In Fig. 3 the empty squares/triangles represent working points for the algorithm with  $q = 8/16$ . In both cases, the critical noise level  $f_c$  is only slightly decreased, but the size of the side information becomes considerably smaller.

## 6. JOINT SOURCE-CHANNEL CODING WITH THE LACK OF SIDE INFORMATION

In this section we describe how the Markovian decoder can be implemented without any transmission of side information. The key points are the special properties of the KS construction (Fig. 2): the first  $k$  rows of  $A$  are characterized by one non-zero element per row and column, where the first  $k$  rows of  $B$  are characterized by 2 non-zero elements. Furthermore, due to the systematic form of  $B$ , each row cannot be written as a linear combination of the other rows. Hence, the first  $k$  bits of the syndrome vector  $z$ , are equal (up to a simple permutation) to the source, with an effective flip rate,  $f_{eff}$ . For  $GF(2)$  for instance,  $z_j = s_i + n_j + n_{j+1}$  ( $i$  marks the position of the nonzero element in the  $j^{th}$  row of  $A$ ), and  $f_{eff} = 2f(1 - f)$ . The first  $k$  symbols of  $z$  are therefore a result of a *hidden* Markov Model (HMM). The underlying transition matrix,  $T$ , generating the source sequence, can be estimated by means of the EM algorithm [18], which is a standard tool for solving such *Parametric Estimation* problems, with linear complexity. Having  $T$  (approximately) revealed, the DBP's can be calculated as described in Eq. (11).

For the general construction of the MN algorithm one adds/subtracts rows of the concatenated matrix  $[AB]$  and the corresponding symbols in  $z$ , such that a situation is finally reached as follows: The first  $k$  rows of  $A$  are the identity matrix, regardless of the construction of the first  $k$  rows of  $B$ . From the knowledge of the noise level  $f$  and the structure of  $i^{th}$  row of  $B$  one can now calculate the effective noise,  $f_{i,eff}$ , of the  $i^{th}$  received source symbol. Since all  $\{f_{i,eff}\}$  are functions of a unique noise level  $f$ , one can estimate the parameters of the Markovian process using some variants of

the EM algorithm. Note, that in the general case the first  $k$  rows of  $B$  contain loops, hence  $\{f_{i,eff}\}$ , are correlated. However, these correlations are assumed to be small as the typical loop size is of  $O(\log(k))$ [19].

## 7. CONCLUDING REMARKS

The only remaining major drawback of the presented decoder is that the complexity (per iteration), scales as  $O(kq^2)$ , this may considerably slow down the decoder even for moderate alphabet size. Note however, that for large  $q$ , such that  $q^2 \geq k$ , and low entropy sequences, the transition matrix,  $T$ , is expected to be very sparse, and dominated by elements of  $O(1)$ . Taking advantage of the sparseness of  $T$ , the complexity of the decoder can be further reduced.

The one-dimensional Markovian decoder can be easily extended to coding of a two-dimensional array of symbols or even to an array of symbols in higher dimensions [13]. The naive complexity of the DBP calculation scales as  $k^d q^{2d+1}$ , where  $k^d$  is the number of blocks in the array, and  $d$  denotes the dimension. Using Markovian and Bayesian assumptions, the complexity can be reduced to  $O(k^d q^2)$ .

## References

- [1] C.E. Shannon: "A mathematical theory of communications," *Bell Syst. Tech. J.*, vol.27, pt.I, pp.379–423; pt.II, pp.623–656, 1948.
- [2] T.M. Cover, J.A. Thomas, "*Elements of information theory*", Wiley. 1991, UK.
- [3] J. Garcia-Frias, Y. Zhao, "Compression of binary memoryless sources using punctured turbo codes", *IEEE Communication Letters*, vol.6, no.9, pp. 394-396, 2002
- [4] R.G. Gallager, *Low Density Parity Check codes*, Research monograph series **21** (MIT press), 1963.
- [5] D.J.C. MacKay, "Good error-correcting codes based on very sparse matrices", *IEEE Transactions on Information Theory*, vol.45, no.2, March 1999, pp.399-431.
- [6] M.C. Davey, D.J.C. MacKay, "Low-density parity check codes over  $GF(q)$ ", *Communications Letters*, vol.2, no.6, June 1998, pp.165-7.
- [7] I. Kanter, H. Rosemarin, "Communication near the channel capacity with the absence of compression: Statistical Mecanical approach", cond-mat-0301005.
- [8] D.J.C. MacKay, M.C. Davey, "Gallager Codes for Short Block Length and High Rate Applications", *Codes, Systems and Graphical Models*, IMA Volumes in Mathematics and its Applications, Springer-Verlag (2000).
- [9] T. Richardson, R. Urbanke, "The capacity of Low-Density Parity-Check codes under message-passing decoding", *IEEE Transactions on Information Theory*, **47**, 599 (2001).
- [10] I. Kanter, D. Saad, "Error-correcting codes that nearly saturate Shannon's bound", *Physical Review Letters*, vol.83, pp.2660-3, no.13 (1999).
- [11] I. Kanter, D. Saad, "Finite-size effects and error-free communication in Gaussian channels". *J. Phys. A*, vol.33, pp.1675-81, no.8 (2000).
- [12] N.S. Skantzos, J. van Mourik, D. Saad and Y. Kabashima, "Average and reliability error exponents in Low-Density-Parity-Check-codes", *J. Phys. A* 36 No 43,11131-11141 (2003).
- [13] I. Kanter, H. Kfir, "An efficient joint source-channel coding for a D-dimensional array" *cond-mat/0308308*.
- [14] I. Kanter, H. Kfir, "Statistical Mechanical Approach to Joint source-channel coding." *Europhys. Lett.* **63**, 310 (2003)
- [15] For the sake of brevity we report  $T$  only for  $q=4$ :
 
$$T = \begin{pmatrix} 0.85 & 0.07 & 0.04 & 0.04 \\ 0.23 & 0.25 & 0.05 & 0.47 \\ 0.47 & 0.05 & 0.25 & 0.23 \\ 0.04 & 0.04 & 0.07 & 0.85 \end{pmatrix} \quad (14)$$
- [16] PPMZ downloaded from [www.cbloom.com/src/ppmz.html](http://www.cbloom.com/src/ppmz.html).
- [17] AC downloaded from [www.cs.mu.oz.au/alistair/arith\\_coder](http://www.cs.mu.oz.au/alistair/arith_coder).
- [18] G.J. McLachlan and T. Krishnan, "The EM Algorithm and Extension". *Wiley Sons, New York*, 1997.
- [19] P. Erdos and A. Renyi, "On the evolution of random graphs", reprinted in J. Spencer (ed) "The art of counting: selected writings", (MIT Press, Cambridge) 1973.